CANONICAL CIRCUIT

PAPER

Thalamo-cortical bouton counts in mouse primary auditory cortex

ABSTRACT

In the primary visual cortex of the cat, thalamocortical synapses constitute about 6% of all asymmetric synapses. While thalamocortical neurons target all cortical layers, the majority are formed in layer 4. For the rat auditory cortex, it has been described that a very substantial portion of the thalamic input also targets lower layer 3, which diverges from the classical thalamocortical innervation pattern described in the cat and primate visual system. Here we described quantitatively the distribution of thalamic afferents across the different layers of mouse auditory cortex and compare the results with data of the cat visual system.

Thalamic axons in the primary auditory cortex (A1) were labelled with an injection of adeno associated viral vector carrying the gene for a green fluorescent protein (GFP) into the medial geniculate body (MGB) of the thalamus of one B6/C57 mouse. After perfusion and immuno-histochemistry, sections with the strongest labeling were identified with conventional fluorescence microscopy and samples were photographed in the confocal microscope using a systematic random sampling scheme. Within those photographs, the labeled boutons were counted by hand. Furthermore, we also automatically counted and averaged pixel intensities in the confocal photographs in order to assess whether they can be used as a simple approximation of the bouton counts.

In the section with strongest thalamic innervation, we found thalamic boutons in all cortical layers, with the largest projection targeting layer 4. Assuming an excitatory synapse density of 1.26×10^9 synapses / mm^3 and that each thalamic bouton forms one synapse in average, we estimate the thalamic bouton density to be 2.74×10^7 boutons / mm^3 in layer 4 in the sections with the strongest labeling (and 1.01, 1.26, 1.29 and 0.96×10^7 in layers 1, 2/3, 5 and 6, respectively). For said section, this implies that 2.74% of the asymmetric synapses in layer 4 of A1 are formed by MGB axons (and 0.73%, 1.02%, 1.33% and 1.06% in layers 1, 2/3, 5 and 6, respectively).

Firstly, this indicates that the distribution of thalamic synapses across layers, in general, and layer 4 as the main site for thalamic innervation, more specifically, in mouse auditory cortex is similar to the cat visual cortex. This may be of relevance for future similar studies, which may be carried out more easily on the mouse. Secondly, our data supports the idea that auditory processing in the cortex relies on an astonishingly small amount of raw auditory information.

Previous study (Costa and Martin, 2009; Douglas and Martin, 2007) estimates that in the cat,

only 6% of all synapses in the visual cortex are thalamo-cortical, and that hence, the remainder must be intracortical. Also, it has been shown that the main target for thalamo-cortical connections in cat visual cortex is layer 4. Costa and Martin (2009) conclude that the primary input site of cat visual cortex is layer 4, and that recurrent connections further process the signal in a *just enough* fashion suggested by Douglas and Martin (2007). They claim that in order for such small input to be efficient in driving the recipient neurons, it has to be synchronised, but also requires intracortical input.

Given that the thalamocortical pathway is such a canonical feature of the sensory neocortex, which so far has been mostly studied in the cat and to some extend in the monkey, we wanted to assess whether there is a difference when compared to a different cortical area in a different animal, like mouse auditory cortex, or if the same morphological and quantitative principles apply. The mouse auditory cortex is particularly interesting, since in a study done by Perella and Costa (2012), all of the thalamic recipient neurons in the cortical layer 4 in the mouse that were reconstructed were found to be pyramidal cells whose dendrites extend to the cortical layers 1, 2 and 3. This is unlike the cat and the monkey visual cortices,in which layer 4 contains a population of spiny stellate cells, whose dendrites project largely within layer 4 (Martin and Witteridge, 1984). Also, while in the cat visual cortex the primary target of thalamic axons is layer 4, in the rat auditory cortex lower layer 3 receives a significant proportion of thalamic innervation, as well (Smith et al, 2012).

Given this anatomical differences between the cat and the mouse, and the complexity of cat experiments, we wanted to:

- assess whether the data from cat visual cortex is comparable to the auditory cortex of the mouse
- to get a quantitative description for the distribution of thalamocortical synapses across all the cortical layers.

This will contribute to both the quantitative and qualitative description of the neural circuitry in said area.

In order to do this, we injected an adeno associated viral vector carrying the gene for a green fluorescent protein (GFP) into the medial geniculate body (MGB) of the thalamus. After perfusion and immuno-histochemistry, sections with the strongest labeling were identified with the fluorescent microscope and random samples photographed in the confocal microscope. Within those photographs, the labeled boutons were counted by hand.

Also, we automatically counted pixel intensities per sample and compared it to the data obtained from counting by hands. In doing so, we wanted to assess whether this method could be used as simple approximation of the effective bouton counts and thus serve as a means to circumvent the time-intensive counting by hand.

MATERIALS AND METHODS

surgical procedures. All experiments, animal treatment, and surgical protocols were carried out with authorisation and under license granted by the cantonal Veterinäramt of Zurich. The data presented here originates from one adult B6/C57 mouse . Anaesthesia was induced with 4%

isoflurane in O_2 and maintained during surgery with 2%-3% isoflurane in O_2.

injection of adeno associated viral vector into MGB. An adeno associated virus, serotype 2/1, carrying the gene for a green fluorescent protein (GFP) unto the expression of CMV promoter was used. The MGB was located using stereotaxic coordinates, and its position verified by recording the neuronal responses to uttered sounds. The adeno associated virus was injected iontophoretically with a current of 2-3 µA (3 seconds on, 3 seconds off) over 15 minutes.

perfusion. After two weeks, the mouse was anaesthetised with a lethal dose of Sodium Pentobarbital (Nembutal) administered intraperitoneally (0.15-0.2 ml). Once there were no responses to pinching, the mice were perfused with a 0.9% NaCl solution, followed by a solution of 4% paraformaldehyde and 0.5% glutaraldehyde (300ml). After fixation, the mice were perfused with a solution of 10% and 20% sucrose IN PB 0.1M. The brains were cut, and the blocks containing the MGB and A1 removed.

histology. To prevent the formation of ice crystals during the freeze-thawing, the brains were further incubated in 30% sucrose in PB overnight. To improve penetration of antibodies the brains were then freeze-thawed in liquid nitrogen t. The brain blocks were then cut at 60 µm and the slices containing the MGB and A1 identified in the light microscope. The selected slices were washed six times in 0.1 PB, followed by three-times wash in PBS/BSA-c.

After that, the slices were alternatively assigned to one of three groups:

- 1 - anti-VGluT2 for light microscopy (LM)
- 2 - anti-VGluT2 for electron microscopy (EM)
- 3 - anti-GFP for EM

The first group was incubated for 3 days in a 1:1000 anti-VGluT2 antibody in PBS/BSA-c solution with 1% Triton at 4°C, then washed three times in PBS/BSA-c and incubated again for 3 hours in a 1:500 anti-guinea-pig alexa fluor 555 antibody in PBS/BSA-c solution with 1% Triton at room temperature. The slices were then washed in PBS and mounted.

The second group was incubated overnight in a 1:5000 anti-VGluT2 antibody in PBS/BSA-c solution at room temperature, then washed three times in PBS/BSA-c and incubated again for 3 hours in a 1:200 Biotin-anti guinea pig antibody in PBS/BSA-c solution at room temperature.

The third group was incubated overnight in a 1:500 anti-GFP antibody in PBS/BSA-c solution at 4°C, then washed three times in PBS/BSA-c and incubated again for 3 hours in a 1:200 Biotin-anti rabbit antibody in PBS/BSA-c solution at room temperature.

After the immunohistochemistry, group 1 and 2 were prepared for the EM as follows: The slices were washed once in PBS and three times in TBS, then incubated overnight in an ABC-kit solution at 4° C. After subsequent washing for ten minutes (three times) in TBS, the peroxidase reaction was induced in the presence of Ni-DAB: The slices were incubated twice for 10 minutes in TB (pH 8), then incubated again for 20 minutes in Ni-DAB (600 mg $NiNH_4SO_4$, 15mg DAB, 100 ml TB pH8). Following this, H_2O_2 was added to the solution to reach a final concentration of

0.005% and the reaction monitored. Finally, the slices were washed in PB, osmicated, embedded and mounted.

selecting samples and counting. Using the light microscope, from the third group described above three slices with the strongest labeling were selected (called 3, 4 and 6). Using a systematic random scheme, 60 to 107 stacks of 30 to 30 to 26.8-73.8 microns were selected for each slice and photographed using confocal microscopy.

All the stacks were grouped according to the slice of origin, with the stacks derived from slice 3 divided into subgroups 3A and 3B. For every group of stacks, an optical disector of 10^3 microns was defined such that the labeling within this disector was clearly visible for every single stack. This was necessary due to the fact that the surface of the slices was wavy as a result of the cutting and hence the photographs taken near the surface unfit. Within those disectors, boutons were counted by hand in fiji according to conventional criteria (varicosity in axon and increase in fluorescence) using TrakEM. To avoid bias towards larger boutons, only boutons were counted that were either completely within the cube or that extended beyond the cube at its left, top and rear borders.

estimating density distribution of thalamic boutons. Under the light microscope, the borders six cortical layers were identified for each of the three slices on the basis of thickness of cortex and neuronal density. Using this identification, the layer of origin was determined for every optical disector. If a disector extended over a layer border, it was assigned to the layer that contained the bulk of it.

In previous studies (Riday, 2012), the synapse density for mouse A1 has been estimated at 1.26 × 10^9 synapses / mm^3. The density for the specific layers are summarised in the table below. In this study, both excitatory and inhibitory synapses were counted. However, in our study, we only want to compare against excitatory synapses, which according to Riday make out 86% of the total.

layer	1	2 / 3	4	5	6	all layers
all synapses × 10^9 per mm^3	1.61	1.44	1.16	1.13	1.05	1.26
excitatory synapses × 10^9 per mm^3	1.39	1.24	1.00	0.97	0.90	1.08

table 1: synapse density for mouse A1 across cortical layers (Riday, 2012)

These numbers have not been corrected for tissue shrinkage, and neither has been our data. We used these numbers to calculate the density of thalamic boutons, assuming that every bouton forms one synapse in average. This is an assumption has been tested in the rat (Smith et al, 2012), but not in the mouse so far (but see discussion).

averaging pixel intensities. With the counting a single disector by hand taking about five minutes, the question naturally arises of how the process can be automatised. Also, it has been shown that counting by hand can be inconsistent even if performed by experienced people.

While a lot of research is done in the field of structure segmentation (Benmansour and Cohen, 2010) and identifying boutons in 2D images (Prodanov et al, 2005), few methods have proven useful in automatically identifying boutons in three dimensional space.

Given that photographs taken in the confocal microscope are automatically corrected to ensure that the light intensity doesn't change in the z-dimension, we run a simple script that computed the average pixel intensity for every stack. Our thesis is that this average value can be used as an approximation for the bouton counts.

The photographs are grayscale, i.e. the pixel values range between 0 and 255. The script was run two times on each section, with the first iteration counting within the 10^3 micron optical disector in which the boutons were also counted by hand (see above), and the second iteration being concerned with a larger section of the data (entire stack in x and y-dimension, and same z-depth as optical disector).

To compare bouton counts and average pixel intensities, KS-tests were performed.

RESULTS

GFP bouton counts distribution. The counts of all the optical disectors were averaged to give a measure of density per layer. Because the absolute counts vary greatly across the four different sections (see discussion and appendix for table) they were were normalised before averaging for the plot below, in order to make the distribution across the sections more comparable.

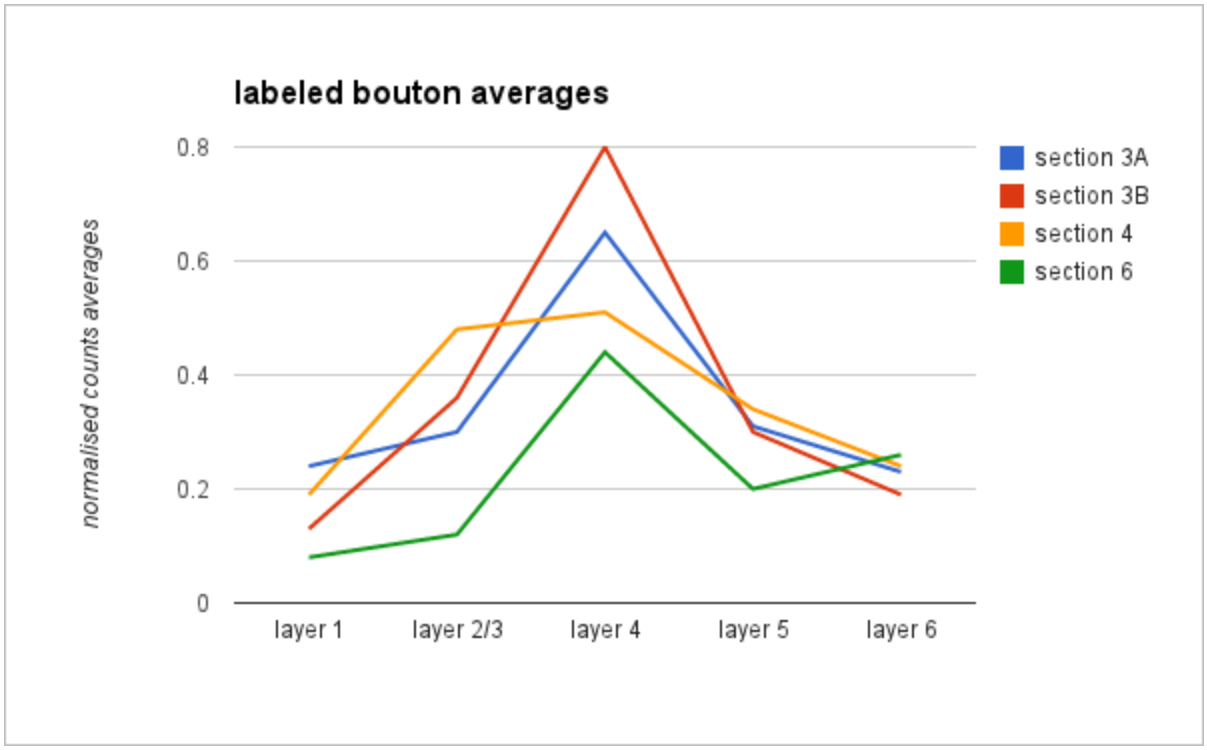

plot 1: boutons counts are normalised by dividing through maximum, then averaged per layer to give a measure of density

Boutons counts were found in all the cortical layers in all the sections, with the highest density of counts found in layer 4.

GFP boutons densities. Due to the variation of counts across the sections, the absolute densities below are calculated on the basis of section 3A and 3B, respectively, where we assume the labeling to be strongest.

layer	1	2/3	4	5	6	all layers
section 3A	1.01×10^7	1.26×10^7	2.74×10^7	1.29×10^7	0.96×10^7	1.36×10^7
section 3B	0.32×10^7	0.90×10^7	2.00×10^7	0.75×10^7	0.48×10^7	0.85×10^7

table 2: labeled bouton counts per mm^3

Again, based on section 3A and 3B, we estimated the percentage of thalamic synapses, based on the data above, the data by Rickey (2012) and the assumption that one bouton corresponds in average to one synapse.

layer	1	2/3	4	5	6	all layers
section 3A	0.7326%	1.0187%	2.7441%	1.3269%	1.0631%	1.3771%
section 3B	0.2347%	0.7267%	2.0048%	0.7718%	0.5260%	0.8528%

table 3: estimate for thalamic synapse percentage

pixel intensities. In order to be able to compare pixel intensities and bouton counts, all the data sets were divided by their respective maximum. The plot below shows the values for section 3A. Pixel intensities I refers to the counts obtained from the disectors, pixel intensites II to the ones obtained from the larger data sets. Refer to appendix for all the data.

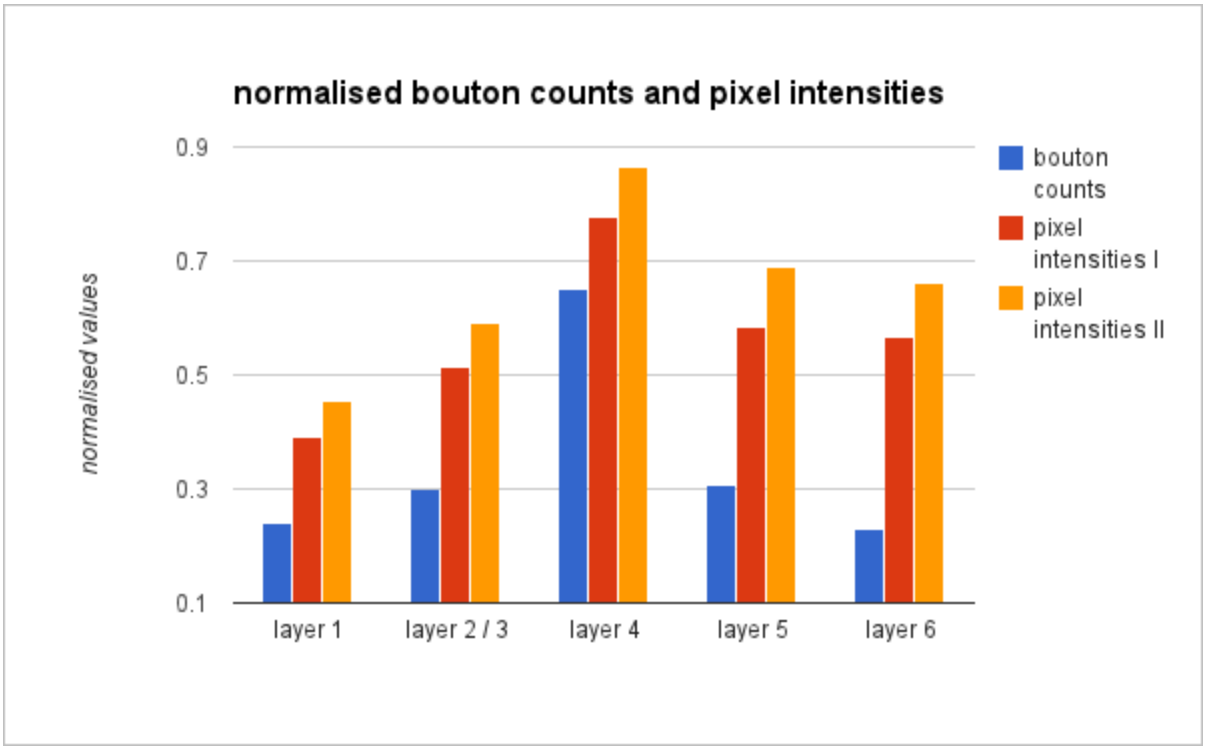

plot 2: bouton counts, pixel intensities for the optical disector and the larger data set, respectively for section 3A. All values normalised by dividing by the maximum

DISCUSSION

GFP bouton counts. The variance of absolute boutons counts across the sections suggests that our labeling did not cover the entire thalamus, and that hence the labeling grew weaker from posterior towards anterior sections.

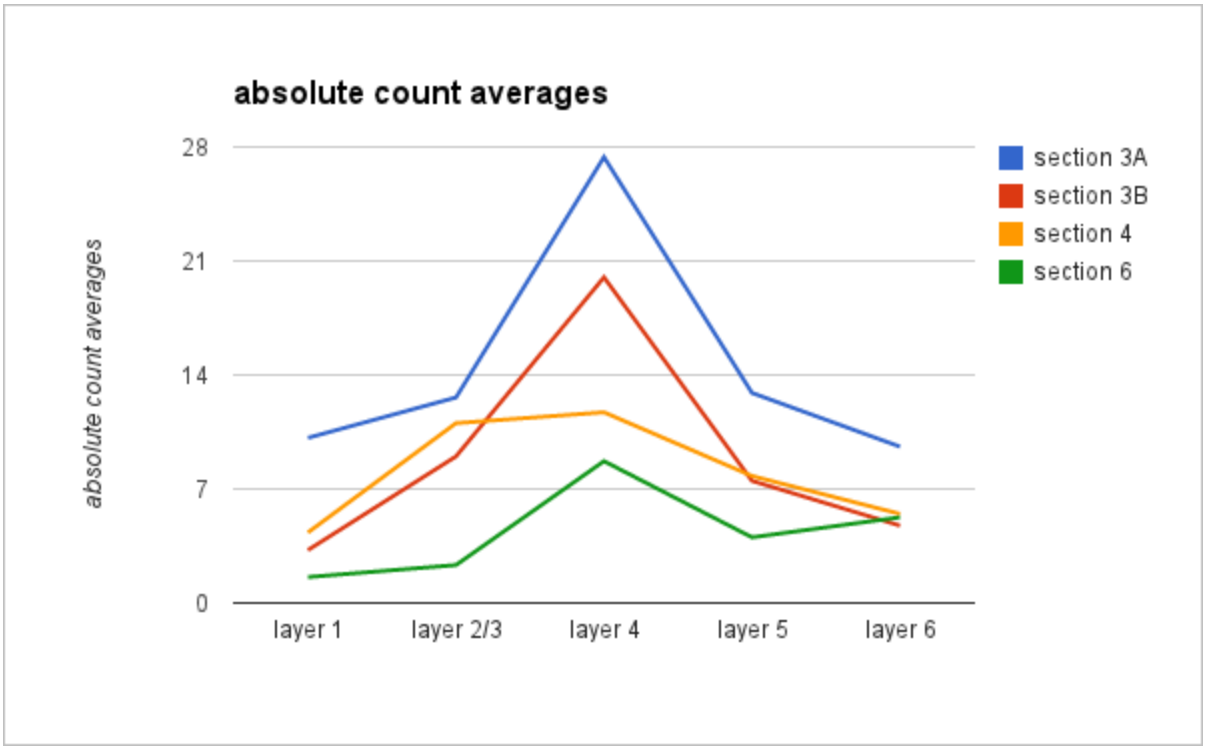

plot 3: absolute counts, averaged per layer

In general, the distribution pattern is consistent across the sections, with two things being particularly striking: Firstly, in section 4, layer 2/3 has a relatively high density of labeled boutons compared to the distribution pattern in the other sections. Indeed, this finding is consistent with the research by Smith et al (2012).

Secondly, in section 6 there is a relatively high density of labeled boutons in layer 6. This maybe due to the fact that section 6 was near the anterior border of A1.

In general, the distribution pattern seems to be similar to the one in the cat.

pixel intensities. While the distribution pattern of pixel intensities seems similar, there is no statistical significant correlation between the manual counts and pixel intensites. Perfoming KS-tests on the pixel intensities from the optical disectors and manual counts yielded D_{max} of 0.6613, 0.7000, 0.7103 and 0.8144 for sections 3A, 3B, 4 and 6, respectively. Those values correspond to P values ranging from 5.6×10^{-24} and 2.6×10^{-56}.

The main issue is that labeled axons also contribute to the pixel intensity. This is especially apparent in layer 6. Consequently, if such a technique was to be used, it would need to be calibrated before by assessing the contribution of axons.

EM. As described above, several slices were prepared during immuno-histochemistry for analysis in the EM. This would have served as a control and allowed to verify our assumption that one bouton forms in average one synapse. However, due to time constraints, the data was

not evaluated.

VGluT. While there is some evidence that the endogenous marker in thalamic boutons called VGluT2 (Nahmani and Erisir, 2005) can be used, the labeling was unsatisfactory when compared to the GFP labeling. This was on one side due to a large amount of false positives (boutons that were labeled by the VGluT antibody, but not by the GFP), and on the other side due to the superficial penetration of the VGluT antibody.

methodological considerations. For the first time, the virus was injected with current. On one hand, this allows for more precise injections. On the other hand, it enabled us to only use one pipette, as both injection and recording could be performed by only one pipette.

LITERATURE CITED

Benmansour F, Cohen LD. 2010. Tubular Structure Segmentation Based on Minimal Path Method and Anisotropic Enhancement. J Comput Vis.

Costa NM, Martin KA. 2009. The Proportion of Synapses Formed by the Axons of the Lateral Geniculate Nucleus in Layer 4 of Area 17 of the Cat. J Comp Neurol 516:264-76.

Douglas R, Martin K. 2007. Recurrent neuronal circuits in the neocortex. Current biology : CB, 17(13), R496–500.

Martin K, Witteridge D. 1984. Form, function and intracortical projections of spiny neurones in the striate visual cortex of the cat. J Physiol 353:463-504.

Nahmani M, Erisir A. 2005. VGluT2 Immunochemistry Identifies Thalamocortical Terminals in Layer 4 of Adult and Developing Visual Cortex. J Comp Neurol 484:458-73.

Perella, Costa NM. 2012. Personal communication.

Prodanov D, Heeroma J, Marani E. 2005. Automatic morphometry of synaptic boutons of cultured cells using granulometric analysis of digital images. Journal of Neuroscience Methods.

Riday C. 2012. Personal communication.

Smith PH, Uhlrich DJ, Manning KA, Banks MI. 2012. J Comp Neurol 520:34-51.

APPENDIX

table 4: absolute, non-normalised bouton count averages per 10 cubic micron per layer and section as mean ± standard deviation, rounded to two significant digits.

	section 3A	**section 3B**	**section 4**	**section 6**

layer 1	10.14 ± 7.54	3.25 ± 2.25	4.33 ± 2.35	1.59 ± 3.26
layer 2/3	12.62 ± 4.45	9.00 ± 3.89	11.04 ± 5.32	2.33 ± 2.00
layer 4	27.38 ± 8.86	20.00 ± 4.24	11.71 ± 3.52	8.71 ± 6.16
layer 5	12.90 ± 4.89	7.5 ± 3.97	7.80 ± 3.03	4.03 ± 2.83
layer 6	9.6 ± 4.85	4.75 ± 2.87	5.47 ± 3.70	5.26 ± 2.96

table 5: normalised bouton count averages per layer and section as mean ± standard deviation, rounded to two significant digits.

	section 3A	**section 3B**	**section 4**	**section 6**
layer 1	0.24 ± 0.18	0.13 ± 0.09	0.19 ± 0.10	0.08 ± 0.16
layer 2/3	0.30 ± 0.11	0.36 ± 0.16	0.48 ± 0.23	0.12 ± 0.10
layer 4	0.65 ± 0.21	0.80 ± 0.17	0.51 ± 0.15	0.44 ± 0.31
layer 5	0.31 ± 0.12	0.30 ± 0.16	0.34 ± 0.13	0.20 ± 0.14
layer 6	0.23 ± 0.12	0.19 ± 0.12	0.24 ± 0.16	0.26 ± 0.15

table 6: normalised pixel intensities for the optical disector

	section 3A	**section 3B**	**section 4**	**section 6**
layer 1	0.39 ± 0.08	0.42 ± 0.04	0.50 ± 0.03	0.34 ± 0.26
layer 2/3	0.51 ± 0.11	0.52 ± 0.07	0.72 ± 0.15	0.58 ± 0.06
layer 4	0.78 ± 0.13	0.80 ± 0.12	0.76 ± 0.12	0.71 ± 0.07
layer 5	0.59 ± 0.09	0.61 ± 0.07	0.71 ± 0.10	0.61 ± 0.07
layer 6	0.57 ± 0.11	0.52 ± 0.05	0.61 ± 0.09	0.74 ± 0.12

table 7: normalised pixel intensities for the larger data set

	section 3A	**section 3B**	**section 4**	**section 6**
layer 1	0.45 ± 0.09	0.48 ± 0.03	0.52 ± 0.03	0.38 ± 0.28
layer 2/3	0.59 ± 0.10	0.57 ± 0.06	0.76 ± 0.15	0.66 ± 0.04
layer 4	0.86 ± 0.09	0.87 ± 0.09	0.81 ± 0.10	0.81 ± 0.08

layer 5	0.69 ± 0.08	0.69 ± 0.08	0.74 ± 0.07	0.71 ± 0.04
layer 6	0.66 ± 0.11	0.57 ± 0.03	0.66 ± 0.10	0.82 ± 0.09

the script used to count pixel intensities

```
import os
from ij import IJ

startZ = 200
endZ = 325
slices = endZ - startZ

startX = 0
endX = 1024
pixelsX = endX - startX

startY = 0
endY = 1024
pixelsY = endY - startY

pixels = pixelsX * pixelsY

folder = DirectoryChooser("Choose source folder").getDirectory() ;

for filename in os.listdir(folder):
   if filename.endswith(".tif"):

      image = IJ.openImage(os.path.join(folder,filename))
      stack = image.getImageStack()

      stackCount = 0

      for z in xrange(startZ , endZ):
         processor = stack.getProcessor(z)
         sliceCount = 0
         for x in xrange(startX, endX):
            for y in xrange(startY, endY):
               sliceCount += processor.get(x, y)

         stackCount += sliceCount
      stackMean = stackCount / float(slices * pixelsX *
      pixelsY)
      print filename , stackMean
```